JOURNAL OF Applied Polymer SCIENCE

Application of Azodiisobutyronitrile and Azobisisoheptonitrile in Low-Density Unsaturated Polyester Resin Manufacturing

Liang-Zhi Guo,[1] Xiao-Jun Wang,[1] Yi-Fan Zhang,[1] Xiao-Yao Wang[2]

[1]College of Materials Science and Engineering, Nanjing University of Technology, Nanjing 210009, China

[2]The Charles E. Via, Jr. Department of Civil and Environmental Engineering, Virginia Polytechnic Institute and State University, Blacksburg, Virginia 24061

Correspondence to: X.-J. Wang (E-mail: xjwang@njut.edu.cn)

ABSTRACT: Low-density unsaturated polyester resin (LDUPR) is an extended application of unsaturated polyester resin (UPR) material. In this study, azodiisobutyronitrile (AIBN) and azobisisoheptonitrile (ABVN) were presented as composite foaming agents and as initiators in LDUPR manufacturing. On the basis of the kinetics of AIBN and ABVN, their optimum half-lives ($t_{1/2}$'s) for LDUPR were both 1.0 h. In this study, the mass ratio of AIBN and ABVN was chosen at 7:3, and the preferred amount of the composite foaming agent was 2 wt % resin. They were treated at a molding temperature of 78.7 ± 1.0°C. The obtained LDUPR had an apparent density of 0.37 ± 0.01 g/cm^3 and a specific compression strength of 35.58 ± 1.50 MPa·g^{-1}·cm^{-3}; it approached the highest specific compression strength value of rigid polyurethane foam (28–35 MPa g^{-1} cm^{-3}). A dual-initiation and dual-foaming mechanism based on the dual-exothermic decomposition properties of the composite foaming agent was proposed with the support of the differential scanning calorimetry and scanning electron microscopy results. In the first stage, ABVN decomposed, released bubble nuclei, and initiated UPR cross-polymerization. The bubble nuclei spread in the resin glue and grew. In the second stage, the gas in resin glue was enriched by the AIBN decomposition. The gelation time of the resin glue was influenced by AIBN and delayed. With the curing of resin, more bubbles grew up, took shape, and were retained in the UPR matrix. © 2013 Wiley Periodicals, Inc. J. Appl. Polym. Sci. **2014**, *131*, 40238.

KEYWORDS: foams; kinetics; resins; thermosets

Received 28 June 2013; accepted 30 November 2013

DOI: 10.1002/app.40238

INTRODUCTION

Low-density unsaturated polyester resin (LDUPR) is an extended application of a composite material based on unsaturated polyester resin (UPR), and it has become one of the most used materials in composite materials development. LDUPR is widely used in the industry, such as auto parts and electrical products.[1–5]

At present, LDUPR is prepared by the introduction of gas into the UPR matrix, and this decreases the density of the cured resin matrix. The chemical foaming method is a useful commercial technology.[6–9] However, the shortcomings of the chemical foaming method are obvious. In the chemical foaming process, the decomposition temperature of a single foaming agent does not match the gelation temperature of the UPR, and the foaming agent does not decompose thoroughly during the UPR curing process.

Azodiisobutyronitrile (AIBN) and azobisisoheptonitrile (ABVN), which are two commercial initiators, are widely used in free-radical polymerization.[10–13] Qin et al.[14] studied the feasibility and properties of UPR cured via microwave irradiation with AIBN. They pointed out that the gelation time was about 20 times shorter than the traditional time. The thermal and mechanical properties of UPR cured with this method were nearly identical to those of UPR initiated in the traditional way. Their studies also indicated that it was easier for AIBN to be excited by microwave irradiation than benzoyl peroxide, 2,5-dimethyl-2,5-di(tert-butylperoxy)hexane, and *tert*-butylhydroperoxide. Kamens[15] pointed out that the foaming of UPR could be carried out with acid-sensitive azo compounds, such as 2-*t*-butylazo-2-hydroxybutane and 1-*t*-butylazo-1-hydroxycyclohexane. Their studies showed that those compounds, such as methacrylonitrile, α-methylstyrene, and laurylmercaptan, could improve the foaming efficiency of UPR based on the weight of resins between 0.001 and 10%. However, there have been few reports on the application of complex azo initiators on UPR. Also, there have been no studies of the dual-initiation and dual-foaming mechanism of azo compounds on LDUPR. During the process of decomposition, AIBN and ABVN decompose into primary radicals and release nitrogen gas. Primary radicals and nitrogen gas are

advantages in LDUPR manufacturing. As for the different foaming activities of AIBN and ABVN, LDUPRs manufactured by AIBN or ABVN may present different properties. In this study, composite foaming agents consisting of various ratios of AIBN and ABVN were put out with the specialties of each foaming agent to improve the properties of LDUPR. Moreover, we optimized the foaming efficiency by choosing AIBN as the major foaming agent and ABVN as the auxiliary one. On the basis of the decomposition kinetics of AIBN and ABVN, three foaming agents, AIBN, ABVN, and their mixtures (with various mass ratios), were applied in LDUPR manufacturing. The optimum composition of the composite foaming agent and the LDUPR manufacturing process were decided on the basis of the optimized properties of the LDUPR. The morphology of the LDUPR was observed by scanning electron microscopy (SEM), and the reaction exotherm in the foaming process was measured by differential scanning calorimetry (DSC). The analytic results show that the dual-initiation and dual-foaming mechanism caused by the composite foaming agent were critical factors to the LDUPR; this was different from that of a single foaming agent action.

EXPERIMENTAL

Materials

The UPR used in this work was P17-902 (obtained from Jinling DSM Resins Co., Ltd., China). It was appropriate for molding under high temperatures. The foaming agents and initiators were AIBN and ABVN (produced by Shanghai No. 4 Reagent & H. V. Chemical Co., Ltd., in China). The nucleating agent of the LDUPR was $CaCO_3$ (obtained from Nanjing Omya Fine Chemical Industry Co., Ltd., China).

Determination of the Decomposition Kinetics

The decomposition kinetics of AIBN and ABVN were observed in a volumetric gas-burette experiment.[16,17] Once the foaming agent began to decompose, the data on gas volume (V_t) were recorded every 10 min, and the maximum value of gas volume (V_{max}) was measured.

Preparation of the Specimens

The LDUPR specimens with the single foaming agent were prepared according to a formula with 100 g of resin, 3 g of nucleating agent, and 1 g of foaming agent, and the molding temperatures (Ts) were set with respect to the half-life ($t_{1/2}$), or half-decay, with values of 0.5, 1.0, 1.5, 2.0, and 2.5 h for a single foaming agent separately.

All of the LDUPR specimens with the composite foaming agent were prepared according to a formula with a mass ratio of 100 g of resin to 3 g of nucleating agent, and the content of the composite foaming agent was varied from 1 to 3% at 0.5% intervals by the weight of UPR. The specimens were cured for 4 h at the proper temperature obtained from the experiment in this study. Then, the specimens were obtained after they cooled down to room temperature. In a parallel experiment, five replicated specimens were tested for each formulation, and the experiment was repeatable.

Property Testing

The gelation time of UPR was measured with a gelation time meter (GT-2, Lin'an Fengyuan Electronics Co., Ltd., China). The apparent density (ρ) was detected according to the international standard ISO 845-2006. The compression strengths of the specimens were measured with an electronic universal testing machine (WDW3100, Changchun Xinke Instrument Co., Ltd., China, maximum pressure = 100 kN and accuracy = 0.5%) according to the international standard ISO 844:2004 ("Rigid Cellular Plastics—Determination of Compression Properties") at the ambient temperature of 23 ± 2°C and a relative humidity of 50 ± 5%.

DSC

A Netzsch DSC204 different scanning calorimeter was used to measure the decomposition exotherm of the composite foaming agent. The specimen was sealed in a volatile aluminum sample pan. Nonisothermal scans were carried out from room temperature to 160°C at a heating rate of 10°C/min under nitrogen conditions. The modulation of temperature for DSC was ±0.1°C. The mass of the composite foaming agent specimen in this experiment was about 20 mg, and sensitivity of DSC was 0.1 μg.

SEM

The specimens were cut to a size of 10 × 10 × 1.5 mm^3. The sections of the samples were observed by SEM (JEOL JSM6500) with a 15-kV accelerating voltage in high-vacuum mode and a magnification of 100 × to investigate the bubbles in the samples. The section surfaces were sputtered with a thin gold layer to enhance the electronic conductivity.

RESULTS AND DISCUSSION

Decomposition Kinetics of AIBN and ABVN

The thermal decomposition of foaming agents is an important factor in the properties of LDUPR. There are differences in the decomposition rate and in the activation energy for the decomposition of various foaming agents.

The decompositions of AIBN and ABVN are first-order reactions,[18,19] and the decomposition constant (k_d) can be evaluated by the equation $\log[V_{max}/(V_{max} - V_t)] = k_d t/2.303$.[20] The volumes of gas released by AIBN (V_t^{AIBN}) and ABVN (V_t^{AIBN}) at regular intervals of time and at the corresponding temperatures are listed in Table I. The thermal decompositions of AIBN and ABVN are shown in Figure 1.

Table I shows that the maximum amount of gas released by AIBN (V_{max}^{AIBN}) was 20.50 ± 0.38 mL (see the data in the sixth column at 80°C in Table I), and the maximum amount of gas given off by ABVN (V_{max}^{AIBN}) was 13.50 ± 0.22 mL (see the data in the fifth column at 70°C and the data in the seventh column at 80°C in Table I). The relation between the value of $\log[V_{max}^{AIBN}/(V_{max}^{AIBN} - V_t^{AIBN})]$ and time is summarized in Figure 2. Also, the relation between the value of $\log[V_{max}^{AIBN}/(V_{max}^{AIBN} - V_t^{AIBN})]$ and time is summarized in Figure 3.

Figure 2 shows that the slopes of the linear fitting equations were 3.19 × 10^{-4}, 9.84 × 10^{-4}, and 3.57 × 10^{-3} min^{-1}; these slopes corresponded to the temperatures 60, 70, and 80°C, respectively. According to the slopes of the three curves shown in Figure 2 and the equation $\log[V_{max}/(V_{max} - V_t)] = k_d t/2.303$, the decomposition rate constants of AIBN at the three different

Table I. Changes in the Amount of Gas Given off by AIBN (V_t^{AIBN}) and ABVN (V_t^{AIBN}) over Time at Different Temperatures

	V_t (mL)					
	$T_1 = 60°C$		$T_2 = 70°C$		$T_3 = 80°C$	
Time (min)	$(V_t^{AIBN})_{60}$	$(V_t^{AIBN})_{60}$	$(V_t^{AIBN})_{70}$	$(V_t^{AIBN})_{70}$	$(V_t^{AIBN})_{80}$	$(V_t^{AIBN})_{80}$
10	0.15 ± 0.01	0.64 ± 0.03	0.46 ± 0.02	1.51 ± 0.05	1.61 ± 0.06	4.68 ± 0.08
20	0.30 ± 0.01	1.25 ± 0.03	0.90 ± 0.03	2.86 ± 0.06	3.11 ± 0.05	7.74 ± 0.11
30	0.43 ± 0.01	1.81 ± 0.04	1.34 ± 0.04	4.05 ± 0.07	4.47 ± 0.06	9.74 ± 0.10
40	0.60 ± 0.02	2.38 ± 0.04	1.78 ± 0.04	5.10 ± 0.07	5.75 ± 0.08	11.00 ± 0.12
50	0.73 ± 0.02	2.90 ± 0.06	2.20 ± 0.05	6.05 ± 0.09	6.90 ± 0.10	11.90 ± 0.13
60	0.92 ± 0.03	3.41 ± 0.05	2.60 ± 0.05	6.88 ± 0.08	8.00 ± 0.12	12.50 ± 0.16
180	2.53 ± 0.05	7.84 ± 0.11	6.86 ± 0.08	11.91 ± 0.12	15.83 ± 0.25	13.50 ± 0.22
300	4.05 ± 0.08	10.33 ± 0.12	10.10 ± 0.14	13.12 ± 0.21	18.75 ± 0.28	13.50 ± 0.22
420	5.44 ± 0.08	11.72 ± 0.10	12.58 ± 0.18	13.50 ± 0.23	19.85 ± 0.36	13.50 ± 0.22
480	6.09 ± 0.10	12.17 ± 0.19	13.60 ± 0.22	13.50 ± 0.23	20.50 ± 0.38	13.50 ± 0.22
540	6.71 ± 0.12	12.50 ± 0.24	14.47 ± 0.26	13.50 ± 0.23	20.50 ± 0.38	13.50 ± 0.22

"T1", "T2", and "T3" represent the three different experimental temperatures in the volumertric gas-burettee experiment

temperatures were obtained, where $(k_d^{60})_{AIBN} = 7.35 \times 10^{-4}$ min^{-1}, $(k_d^{70})_{AIBN} = 2.27 \times 10^{-3}$ min^{-1}, and $(k_d^{80})_{AIBN} = 8.23 \times 10^{-3}$ min^{-1}. Furthermore, the decomposition rate constants of ABVN at the three different temperatures was also obtained in the same way, where $(k_d^{60})_{ABVN} = 4.83 \times 10^{-3}$ min^{-1}, $(k_d^{70})_{ABVN} = 1.19 \times 10^{-2}$ min^{-1}, and $(k_d^{80})_{ABVN} = 4.26 \times 10^{-2}$ min^{-1}.

The decomposition rate constant of the foaming agent followed the Arrhenius equation at different temperatures:

$$k_d = A_d e^{-Ed/RT}$$

where A_d is the frequency factor, E_d is the activating energy of the foaming agent decomposition, and R is the molar gas constant. When we took the log of the equation and the matrix expression, we obtained:

$$\begin{bmatrix} \frac{1}{T_1}1 \\ \frac{1}{T_2}1 \\ \frac{1}{T_3}1 \end{bmatrix} \begin{bmatrix} -\frac{E_d}{R} \\ \ln A_d \end{bmatrix} = \begin{bmatrix} \ln A_d^{60} \\ \ln A_d^{70} \\ \ln A_d^{80} \end{bmatrix}$$

When $(k_d^{60})_{AIBN}$, $(k_d^{70})_{AIBN}$, and $(k_d^{80})_{AIBN}$ or $(k_d^{60})_{ABVN}$, $(k_d^{70})_{ABVN}$, and $(k_d^{80})_{ABVN}$ were incorporated into the matrix expression, the solutions could be found for each one, such as $E_d^{AIBN} = 127.9$ kJ/mol, $\ln A_d^{AIBN} = 38.9$ for AIBN, and $E_d^{ABVN} = 121.5$ kJ/mol, and $\ln A_d^{ABVN} = 38.5$ for ABVN. With the previous results, the decomposition rate constant for temperature could be obtained from the equations $\ln k_d^{AIBN} = 38.9–1.538 \times 10^4/T$ and $\ln k_d^{AIBN} = 38.5–1.461 \times 10^4/T$. It was revealed that the decomposable activation energy of ABVN ($E_d^{AIBN} = 121.5$ kJ/mol) was lower than that of AIBN ($E_d^{AIBN} = 127.9$ kJ/mol), and ABVN decomposed more rapidly than AIBN at the same temperature. Therefore, the initiation efficiency of ABVN was higher than that of AIBN in the UPR system.

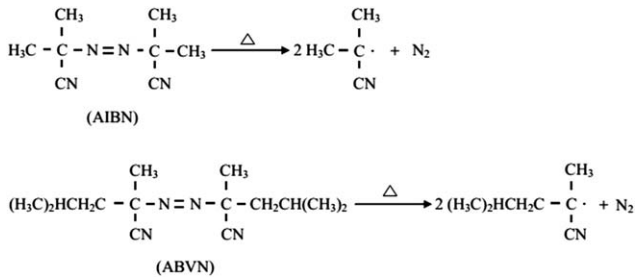

Figure 1. Thermal decomposition of AIBN and ABVN.

Effect of a Single Foaming Agent on the Properties of LDUPR

The decomposition rate of AIBN or ABVN was different at the same temperature. According to the expression $R_d = -d[I]/dt = k_d[I]$, the decomposition rate (R_d) and the concentration

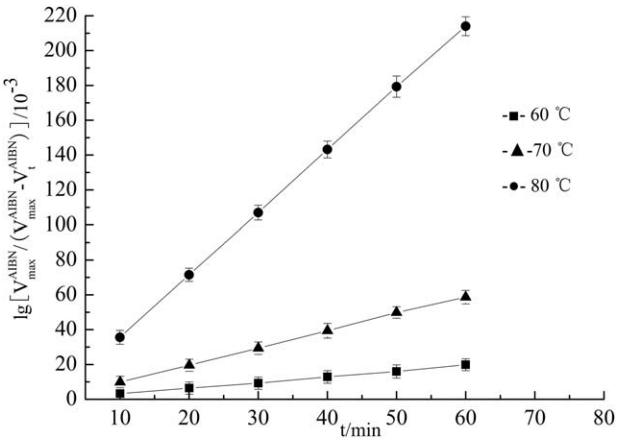

Figure 2. Relationship between the value of $\log[V_{max}^{AIBN}/V_{max}^{AIBN} - V_t^{AIBN})]$ and the time (t) for AIBN decomposition.

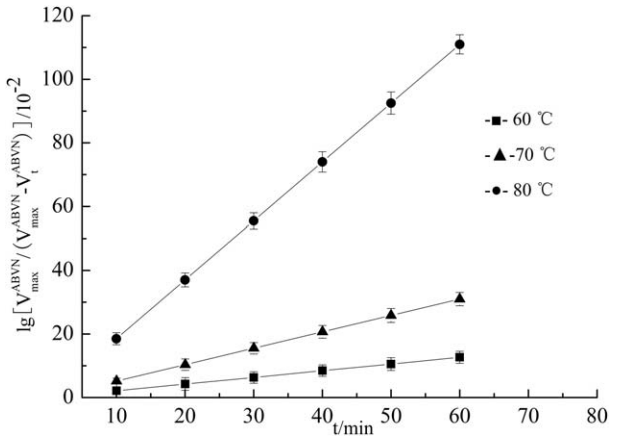

Figure 3. Relationship between the value of $\log[V_{max}^{AIBN}/(V_{max}^{AIBN} - V_t^{AIBN})]$ and the time (t) for ABVN decomposition.

of foaming agents ([I]) were an integral expression: $\ln [I]/[I]_0 = -k_d t$, where $[I]_0$ is the initial concentration of foaming agent. When the concentration of the foaming agents decreased to the half of $[I]_0$, the $t_{1/2}$'s were matched to the changed equation $t_{1/2} = \ln 2/k_d$, acquired from the expression of $\ln [I]/[I]_0 = -k_d t$. When we combined the two expressions $t_{1/2} = \ln 2/k_d$ and $\ln k_d^{AIBN} = 38.9–1.538 \times 10^4/T$, the $t_{1/2}^{AIBN}$ of AIBN at a regular temperature could be calculated. The $t_{1/2}$ of ABVN at a regular temperature could be calculated by the combination of the two expressions $t_{1/2} = \ln 2/k_d$ and $\ln k_d^{AIBN} = 38.5–1.461 \times 10^4/T$. The corresponding Ts are listed in Table II with respect to $t_{1/2}$'s of 0.5, 1.0, 1.5, 2.0, and 2.5 h for both AIBN and ABVN. The properties of the LDUPR specimen containing AIBN and ABVN with 100 g of resin, 3 g of nucleating agents, and 1 g of foaming agent are also listed in Table II.

Table II shows that that ρ of LDUPR was the lowest when the $t_{1/2}$ was 1.0 h for either AIBN or ABVN. This was caused by the coincidence of the foaming agent decomposition and the curing of UPR when $t_{1/2}$ was 1.0 h. When $t_{1/2}$ was less than 1.0 h, the amounts of free-radical $C(CH_3)_2C$ decomposed by AIBN or the amounts of free-radical $(CH_3)_2CHCH_2(CH_3)_2C$ decomposed by ABVN were higher. Higher amounts of free-radical initiated a higher curing rate of resin glue compared to that of the gas dissolving in resin glue, and less gas dissolution indicated a higher ρ of LDUPR.

When the $t_{1/2}$ value of AIBN or ABVN was longer than 1.0 h, the liberation of the free initial group became slower, and even the concentration of the free initial group was decreased. A lower content of the free-radical made the polymerization of the resin slower, and the viscosity of the resin glue was lower, the bubbles collapsed, and the ρ of LDUPR were higher too. As the activity of AIBN was weaker than that of ABVN,[21] more gas could dissolve in the resin before it cured. Table II also shows that when AIBN and ABVN had the same value of $t_{1/2}$, the apparent densities of the specimens with AIBN were lower than those with ABVN.

Effects of the AIBN/ABVN Composite Foaming Agent on the Properties of LDUPR

The previous study showed that at the same content of single foaming agent (1.0 g/100 g of resin), the apparent density of LDUPR with AIBN (ρ_{AIBN}) was lower than that of LDUPR with ABVN (ρ_{ABVN}) at different $t_{1/2}$ values ($t_{1/2} = 0.5$, 1.0, 1.5, 2.0, and 2.5 h, respectively). Therefore, AIBN was selected as the major foaming agent, and ABVN was selected as the auxiliary one.

In this study, a composite foaming agent was constructed by AIBN and ABVN at various mass ratios of 5:5, 6:4, 7:3, 8:2, and 9:1. A low density was the first factor of concern for LDUPR, and the specific compression strength was the second factor and needed to be kept at a high value for LDUPR. Table II shows that the specimen with the lowest density corresponded to $t_{1/2} = 1.0$ h under a higher specific compression strength. Therefore, $t_{1/2} = 1.0$ h was considered to be the optimum $t_{1/2}$ value, and the curing temperature of LDUPR was set to match $t_{1/2} = 1.0$ h for the composite with a foaming agent.

From the equation $t_{1/2} = \ln 2/k_d$, the expression of the decomposition rate constant of AIBN was expressed as $\ln k_d^{AIBN} = 38.9–1.538 \times 10^4/T$, and the expression of the decomposition rate constant of ABVN was $\ln k_d^{AIBN} = 38.5–1.461 \times 10^4/T$. The relation between $t_{1/2}$ and the temperature (T) was deduced as $\log t_{1/2} = E/T - F$, where E and F are constants. Therefore, $t_{1/2}^{AIBN}$ was calculated as $\log t_{1/2}^{AIBN} = 5845.7/T - 16.6$, and the $t_{1/2}$ of ABVN ($t_{1/2}^{AIBN}$) was calculated from $\log t_{1/2}^{AIBN} = 6338.4/T - 18.8$ according to the $t_{1/2}$ at different temperatures. Once the composite foaming agent was constructed by AIBN and ABVN, the $t_{1/2}$ of the composite foaming agent could be obtained as $t_{1/2C}\sqrt{I_C} = t_{1/2A}\sqrt{I_A} + t_{1/2B}\sqrt{I_B}$, where $t_{1/2A}$, $t_{1/2B}$, and $t_{1/2C}$ are the half-live values of foaming agent A, foaming agent B, and composite foaming agent C, respectively,

Table II. Properties of LDUPR with a Single Foaming Agent with Different $t_{1/2}$'s

	T (°C)		ρ (g/cm^3)		σ (10% deformation; MPa)		σ_S (MPa g^{-1}·cm^{-3})	
$t_{1/2}$ (h)	T_{AIBN}	T_{ABVN}	ρ_{AIBN}	ρ_{ABVN}	σ_{AIBN}	σ_{ABVN}	σ_s^{AIBN}	σ_s^{AIBN}
0.5	87.2 ± 1.0	72.5 ± 1.0	0.54 ± 0.02	0.65 ± 0.01	15.35 ± 0.75	17.92 ± 0.82	28.32 ± 1.42	27.40 ± 1.28
1.0	81.5 ± 1.0	66.9 ± 1.0	0.53 ± 0.01	0.62 ± 0.01	15.80 ± 0.74	18.44 ± 0.79	30.10 ± 1.37	29.69 ± 1.35
1.5	78.3 ± 1.0	63.7 ± 1.0	0.56 ± 0.02	0.67 ± 0.02	16.66 ± 0.85	19.37 ± 0.95	29.59 ± 1.45	29.00 ± 1.42
2.0	76.0 ± 1.0	61.5 ± 1.0	0.60 ± 0.02	0.70 ± 0.01	17.52 ± 0.83	20.95 ± 0.82	29.40 ± 1.39	29.84 ± 1.44
2.5	74.2 ± 1.0	59.8 ± 1.0	0.61 ± 0.02	0.71 ± 0.02	18.42 ± 0.88	21.10 ± 0.80	30.30 ± 1.46	29.59 ± 1.39

σ, compressive strength; σ_S, specific compressive strength.

Table III. Properties of LDUPR with a Composite Foaming Agent with Different Mass Ratios and a $t_{1/2}$ of 1.0 h

AIBN/ABVN	T (°C)	ρ (g/cm^3)	σ (10% deformation; MPa)	σ_S (MPa·g^{-1}·cm^{-3})
5:5	75.7 ± 1.0	0.52 ± 0.02	15.52 ± 0.65	29.85 ± 1.49
6:4	78.1 ± 1.0	0.46 ± 0.01	14.74 ± 0.59	31.90 ± 1.54
7:3	78.7 ± 1.0	0.42 ± 0.01	13.76 ± 0.43	32.68 ± 1.57
8:2	78.9 ± 1.0	0.50 ± 0.01	15.61 ± 0.62	31.41 ± 1.28
9:1	79.2 ± 1.0	0.51 ± 0.02	15.15 ± 0.70	29.82 ± 1.36

σ, compressive strength; σ_S, specific compressive strength.

Table IV. Properties of LDUPR with Different Contents of the Composite Foaming Agent

Content of the foaming agent (g/100 g of resin)	ρ (g/cm^3)	σ (10% deformation; MPa)	σ_S (MPa g^{-1}·cm^{-3})
1.0	0.42 ± 0.01	13.76 ± 0.45	32.68 ± 1.63
1.5	0.41 ± 0.01	13.58 ± 0.53	32.80 ± 1.58
2.0	0.37 ± 0.01	12.99 ± 0.46	35.58 ± 1.50
2.5	0.39 ± 0.02	13.53 ± 0.55	34.96 ± 1.64
3.0	0.40 ± 0.02	12.82 ± 0.48	31.89 ± 1.55

σ, compressive strength; σ_S, specific compressive strength.

and I_A, I_B, and I_C are the concentrations of A, B, and C, respectively.

To define the optimum composition of a composite foaming agent, the mass ratios of the resin, $CaCO_3$, and composite foaming agent was set at 100:3:1. The curing temperature was set to match the $t_{1/2}$ value of the AIBN/ABVN composite foaming agent ($t_{1/2} = 1.0$ h). The effects of the different compositions of the composite foaming agents on the curing temperatures and the properties of LDUPR are listed in Table III.

It is summarized in Table II and Table III that the apparent density of LDUPR with the composite foaming agent was lower than that of LDUPR with a single foaming agent with the same addition of foaming agent. Also, the LDUPR specimen had the lowest apparent density and a higher specific compression strength when the mass ratio of AIBN and ABVN was 7:3, as indicated in Table III.

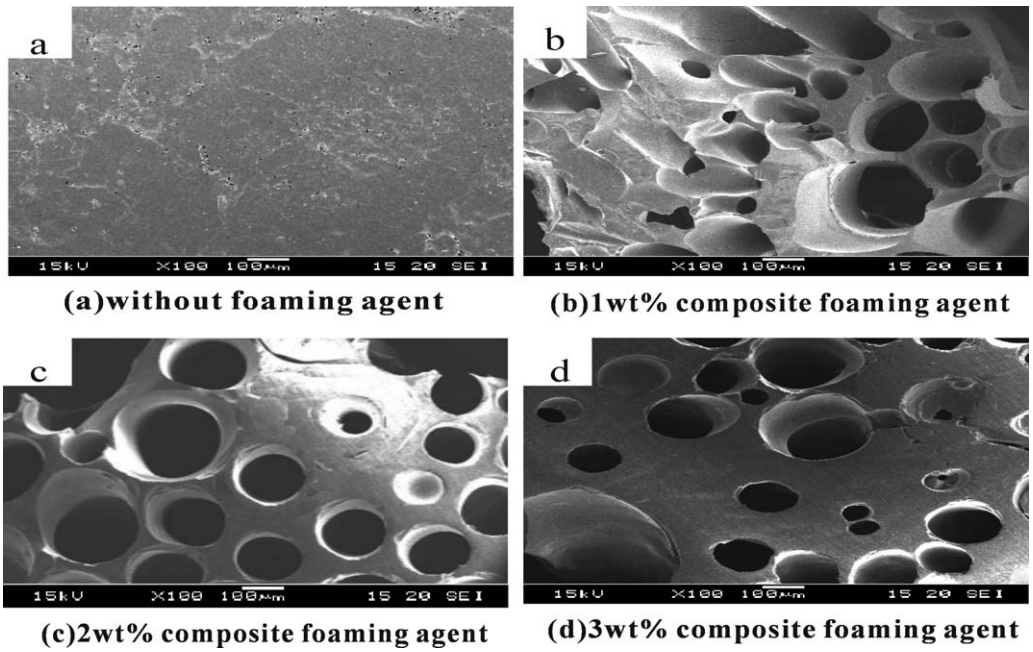

Figure 4. SEM micrographs of LDUPR with different contents of the composite foaming agent.

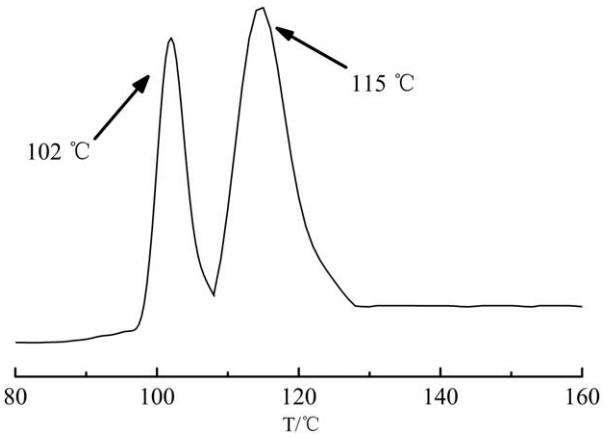

Figure 5. DSC thermogram of the AIBN/ABVN composite foaming agent with a mass ratio of 7:3 (T = temperature).

The content of the composite foaming agent was a critical factor that affected the properties of LDUPR. In this study, where the composite foaming agent was in the mass ratio of 7:3 for AIBN/ABVN, the effects of the composite foaming agent on the properties of LDUPR were studied. The T was set at 78.7 ± 1.0°C with respect to a $t_{1/2}$ of 1.0 h. In practice, the addition of a foaming agent is usually done at lower than 3.0 wt % of the resin, and the addition of the nucleating agent is usually controlled at lower than 5.0 wt % of the resin.[22] Therefore, the addition of the composite foaming agent was set from 1.0 to 3.0 wt % at 0.5% intervals of UPR, and the addition of $CaCO_3$ used as the nucleating agent was set at 3.0 wt % of UPR.

The effects of the composite foaming agent at various additions on the apparent density and specific compression strength are listed in Table IV. Table IV shows that the optimal addition of the composite foaming agent was at 2.0 wt % of UPR and corresponded to the lowest apparent density of 0.37 ± 0.01 g/cm^3 and the highest specific compression strength of 35.58 ± 1.50 MPa g^{-1}·cm^{-3} for LDUPR. The specific compression strength of LDUPR was higher than that of the rigid polyurethane foam (28–35 MPa g^{-1}·cm^{-3}).[23]

Table IV also shows that both the apparent density and the compression strength of the LDUPR specimen decreased when the addition of the composite foaming agent increased from 1.0 to 2.0 wt % of UPR. This was caused by the increase in the bubble amounts when the addition of the composite foaming agent changed from 1.0 to 2.0 wt %. This change was proven by the SEM micrographs of the specimens with composite foaming agents and compared with the UPR specimens without foaming agent [Figure 4(a)]. The amounts of bubbles with the composite foaming agent at 1.0 wt % of UPR [Figure 4(b)] were less than those at 2.0 wt % [Figure 4(c)], and the distribution of bubbles was less homogeneous. When the addition of the composite foaming agent changed to more than 2.0 wt % of UPR, the apparent density of the LDUPR increased. We deduced that the gelation process of the UPR was accelerated by the increase of radicals, and the growth of the bubble was stunted. As shown in Figure 4(d), because the larger bubbles were broken down, the compression strength of the LDUPR specimens with the foaming agent at 3.0 wt % was decreased because of the irregular and inhomogeneous bubble structure.

Analysis of the Composite Foaming Agent Mechanism for Preparing LDUPR

A dual-initiation and dual-foaming mechanism based on the dual-exothermic decomposition properties of the composite

Table V. Gelation Times and Peak Temperatures of UPR Initiated by AIBN, ABVN, and AIBN/ABVN

Initiator	Content (g/100 g of resin)	$t_{1/2}$ (h)	T (°C)	Gelation time (min)	Peak temperature (°C)
AIBN	2.0	1.0	81.5 ± 1.0	74 ± 0.8	263 ± 5
ABVN	2.0	1.0	66.9 ± 1.0	46 ± 0.5	296 ± 8
AIBN/ABVN = 7:3 (with mass ratio)	2.0	1.0	78.7 ± 1.0	66 ± 0.6	279 ± 6

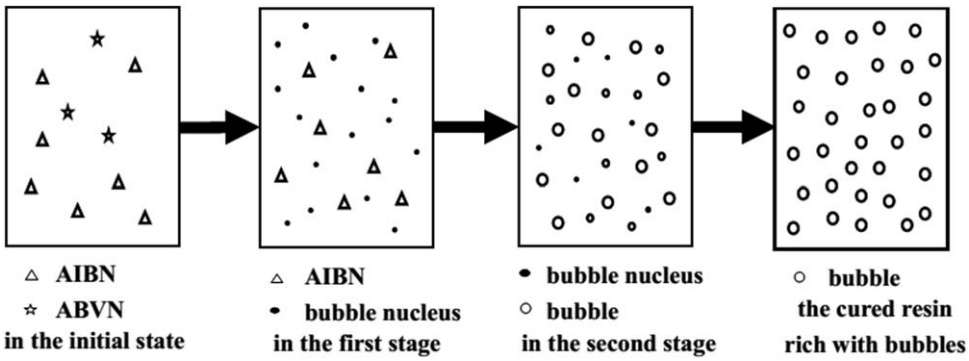

Figure 6. Dual-foaming mechanism of the composite foaming agent for UPR (a) in the initial state, (b) in the first stage, and (c) in the second stage and (d) the cured resin rich with bubbles.

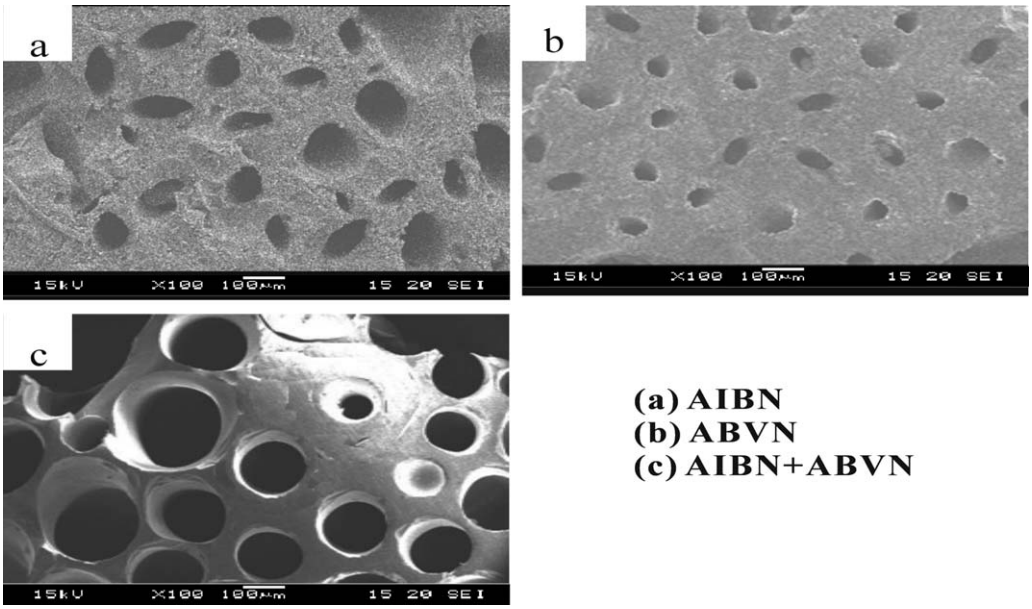

Figure 7. SEM micrographs of LDUPR with different kinds of foaming agents.

foaming agent was proposed with the support of the DSC results. Figure 5 shows the dual-exothermic decomposition of the composite foaming agent. From the DSC curve, the decomposition of the composite foaming agent shows two exotherm stages: ABVN decomposed in the first exothermic stage, and later, AIBN decomposed. With the rise in temperature, ABVN decomposed from 98 to 112°C in the first stage, released bubble nuclei, and also initiated UPR cross-polymerization. The bubble nuclei spread in the resin glue and the viscosity of the resin glue was a little higher.

In the second stage, the major foaming agent AIBN decomposed from 106 to 132°C. AIBN not only acted as a foaming promoter but also impelled the tiny bubble nuclei to grow in the resin glue. The decomposition of AIBN enriched the gas in the resin glue. Meanwhile, the gelation time of the resin glue was influenced by AIBN and delayed. As the proper prolongation of the gelation time of resin glue changed to 66 ± 0.6 min (in Table V), the viscosity increase of the resin glue slowed. A slower viscosity increase in the resin glue was beneficial to the bubble growth and prevented the bubble from escaping from the resin glue. With the curing of the resin, the bubbles grew, took shape, and were retained in the LDUPR matrix. The dual-foaming process determined that the resin glue was rich with bubbles before resin glue was cured, and this process is described in Figure 6. The dual-initiation and dual-foaming mechanism put forward in this study is different from that of a single foaming agent presented before and is suitable for UPR being foamed and initiated.

As for the single foaming agent of AIBN, the gelation time was longer and the collapse of the bubbles occurred. In this condition, the bubbles became flat and took the flat shape shown in Figure 7(a). On the other hand, the gelation time was shorter with the existence of the single agent ABVN and resulted in the gas dissolving in the resin glue incompletely. So, the solid between two adjacent bubbles was obvious, and this phenomenon is shown in Figure 7(b). The gelation times of the resin glue with AIBN, ABVN, and AIBN/ABVN were detected and summarized in Table V.

Table V shows that the gelation time of the resin glue with the AIBN/ABVN composite foaming agent was between that of AIBN and that of ABVN. The gelation time of the resin glue with the composite foaming agent was slightly longer than the $t_{1/2}$ of the foaming agent ($t_{1/2} = 1.0$ h), and this promoted bubble homogenous distribution in the resin matrix [see Figure 7(c)]. The bubbles in the resin matrix were in a perfect state, and this decreased the density of LDUPR.

CONCLUSIONS

According to the exotherm and decomposition specialties of AIBN and ABVN, they could be mixed as composite foaming agents and initiators for LDUPR. The optimum mass ratio of the composite foaming agent for AIBN and ABVN was 7:3. At a T of 78.7 ± 1.0°C, the LDUPR manufactured with the composite foaming agent at 2.0 wt % of the resin presented an apparent density of 0.37 ± 0.01 g/cm^3, a compression strength (with 10% deformation) of 12.99 ± 0.46 MPa, and a specific compression strength of 35.58 ± 1.50 MPa·g^{-1}·cm^{-3}. The specific compression strength of LDUPR approached that of the highest value of rigid polyurethane.

A dual-initiation and dual-foaming mechanism based on the dual-exothermic decomposition properties of the composite foaming agent was proposed with the support of DSC and SEM; this was different from that of a single foaming agent. In the first stage, ABVN decomposed, released bubble nuclei, and initiated the UPR cross-polymerization. The bubble nuclei spread in the resin glue, and the viscosity of the resin glue was higher. In the second stage, the gas in resin glue was enriched by the AIBN decomposition and the gelation time of the resin glue was influenced by AIBN and delayed. With the curing of

resin, more bubbles grew, took shape, and were retained in the LDUPR matrix.

ACKNOWLEDGMENTS

The authors thank Jinling DSM Resin Co., Ltd., for supplying materials; the foundation of the Priority Academic Program Development of Jiangsu Higher Education Institutions (contract grant number PAPD 2011-6); and the Open Experimental Foundation of Nanjing University of Technology (contract grant number NJUTKF2012012).

REFERENCES

1. Carlisle, K. B.; Gadysz, G. M.; Chawla, K. K. *J. Cell. Polym.* **2007**, *3*, 157.
2. Brent, S. M. *Curr. Opin. Colloid Interface Sci.* **2007**, *12*, 232.
3. Erwin, M. W.; Freddy, Y. C. B.; Xiao, H. *Compos. Sci. Technol.* **2005**, *65*, 1840.
4. Ferreira, J. A. M.; Salviano, K.; Costa, J. D. *J. Mater. Sci.* **2010**, *13*, 3547.
5. Lorenzo, B.; Francesco, G. *Int. J. Solids Struct.* **2001**, *38*, 7235.
6. Rong, G.; Biqin, W.; Deping, L.; Quan, F.; Banglong, X. *J. Appl. Polym. Sci.* **2004**, *93*, 1698.
7. Yihe, Z.; Bo, L.; Fengzhu, L.; Wenmin, G. *J. Appl. Polym. Sci.* **2012**, *2*, 756.
8. Chong, H. L.; Ki, J. L.; Ho, G. J.; Seong, W. K. *Adv. Polym. Tech.* **2000**, *2*, 97.
9. Qingxiu, L.; Laurent, M. M. *J. Appl. Polym. Sci.* **2003**, *14*, 3139.
10. Masahide, T.; Yui, N.; Toshihiro, T. *Chem. Phys. Lett.* **2000**, *332*, 503.
11. Xiang, F.; Xue, Y. Y.; Xian, J. Y. *Tetrahedron* **2007**, *63*, 10684.
12. Fu, Y.; Song, H. H.; Zhou, C.; Sun, S. L. *Polym. Compos.* **2013**, *1*, 15.
13. Katsukiyo, I. *J. Polym. Sci. Polym. Chem. Ed.* **1971**, *9*, 2541.
14. Qin, Y.; Huang, Z. T.; Yang, G. R. *Thermosetting Resin* **2006**, *21*, 14.
15. Kamath, V. R.; Kamens, E. R. U.S. Pat. 4167613 (**1979**).
16. Elprince, A. M.; Mohamed, W. H.; El-Wakil, E. M. *Soil Sci. Am. J* **2008**, *1*, 83.
17. Neiner, D.; Karkamkar, A.; Bowden, M.; Choi, Y. J.; Luedtke, A.; Holladay, J.; Fisher, A.; Szymczak, N.; Autrey, T. *Energy Environ. Sci.* **2011**, *10*, 4187.
18. Nuyken, O.; Dauth, J.; Pekruhn, W. *Angew. Makromol. Chem.* **1991**, *3*, 207.
19. Miao, J. G.; Cheng, Z. M.; Zhou, M. H.; Pan, D. *J. Macromol. Sci. A* **2012**, *10*, 869.
20. Edward, L. M. C. Laboratory Preparation for Macromolecular Chemistry; McGraw: New York, **1970**.
21. Jitendra, S. S.; Shrikant, A. B.; Sanjay, G. *Polymer* **2005**, *25*, 11451.
22. Chul, B. P.; John, J. B. *Polym. Eng. Sci.* **1998**, *11*, 1862.
23. Harpal, S.; Jain, A. K. *J. Appl. Polym. Sci.* **2009**, *2*, 1115.